PALAEOCURRENT TRENDS IN THE KIRKI-ESSIMI TERTIARY BASIN, N.E. GREECE, AS SUGGESTED BY MAGNETIC FABRIC INVESTIGATIONS.

Christos Spaïs[1]

Department of Geology,
The University,
Southampton SO9 5NH,
England.

SUMMARY.

The sedimentary sequence of the Kirki-Essimi basin and the Drymou-Melias Series (at the eastern margin of the basin) were sampled at 16 locations for Palaeomagnetic and Magnetic Fabric investigations. The basin occurs at the southern margin of the Rhodope Massif and is Tertiary in age.

Measurements of the Anisotropy of the Magnetic Susceptibility (Magnetic Fabric) were carried out on a total of 400 specimens from the above sampling sites, using a Low Field Torque Magnetometer (LFTM).

The primary style depositional Magnetic Fabric exhibited by the majority of the sites allowed the estimation of palaeocurrent directions in the basin area.

Two main palaeocurrent trends emerge, approximately N-S and E-W, mainly typified by sites situated in the western and central parts of the basin respectively.

The sedimentological and geological implications of these two main inferred palaeocurrent trends are summarized in terms of basin infilling.

1. INTRODUCTION - GEOLOGICAL BACKGROUND.

The estimation of the prefered grain orientation in clastic sediments from the Anisotropy of their Magnetic Susceptibility is a quick and accurate method of finding ancient current directions. Hamilton and Rees (1970 and 1971) suggested how to interpret a given sedimentary magnetic fabric and provided the stimulus for the use of the method in sedimentological studies. The method has been widely used in the investigation of palaeocurrents in sedimentary basins (Crimes and Oldershaw, 1967; Hamilton and Loveland, 1967; Rees et.al., 1968; Von Rad, 1971; Aziz-ur-Rahman et al., 1975).

The principal objective of this study relates to the appraisal of the anisotropy of the magnetic susceptibility of the sediments in order to delineate possible palaeocurrent trends within the Kirki-Essimi basin. Such a study has a potential to show possible palaeoslope positions too. As there

is some geological evidence that the disseminated-stratiformal mixed-sulphide mineralization is controlled by sedimentary structures, knowledge of palaeoslopes is relevant to recognision of these parts of the basin where penecontemporeneous mass movement of sediment has taken place.

The location of the area of this study in N.E. Greece is shown in Fig.1. It has an areal extent of approximatelly 250 km² and is situated to the north of the city of Alexandroupolis.

Geologically, the area comprises mainly the Kirki-Essimi basin, which is one of a number of Tertiary extensional volcano-sedimentary basins, which occur on the southern margin of the crystalline basement of the Rhodope massif. The present outcrop of the Kirki-Essimi basin has an elongated shape with its long axis trending approximately E-W for 25 km and its short axis roughly N-S, for 10 km.

At its eastern margin the basin lies unconformably on the Drymou-Melias series, while its western margin is concealed beneath a cover of Neogene and Quaternary sediments. The sedimentary rocks which form its northern boundary lie unconformably on the older crystalline metamorphic rocks of the Rhodope basement. At its southern margin, the volcanosedimentary rocks of the basin are separated from an Eocene basal unit of breccia-conglomerate by a major E-W trending fault. Penecontemporeneous movement along this fault has been an important factor in the development of the basin. At the south-western edge of the basin, south of the village of Kirki, another group of metamorphic rocks occurs, known as the "Phyllite series". This series together with the Drymou-Melias series constitute the Circum Rhodope belt. It is a unit of low grade metamorphic rocks and is considered by Papanikolaou (1984) to be thrust onto the Rhodope Massif.

Metamorphic rocks constitute the main group of rocks within the Rhodope Massif proper. The metamorphic rocks of the eastern Rhodope Massif can be subdivided into two major units (Billett and Nesbitt, 1986), the Crystalline Gneiss unit and the Amphibolite and Serpentinite unit.

The Drymou-Melias Series is a volcanosedimentary series of 800-900 m in thickness comprising mainly shale, marl, sandstone, greywacke, and pyroclastic rocks. There is much controversy as to whether the Series is of Middle Eocene or Upper Cretaceous age (Katirtzoglou et al., 1981).

It is believed (Katirtzoglou et al., 1981) that the Kirki-Essimi basin was formed by reactivation along older fault lines with a mainly E-W trend, primarily developing as a pull-apart basin (Sanderson et al, 1986) on the southern flanks of the Rhodope Massif. Jacobshagen (1977) suggests that the basin was created after an intense orogenic phase during Eocene times, which affected the whole Internal Hellenides area. Three main groups of rocks occur within the basin:

i. A marine sedimentary sequence of argillites and arenites.
ii. Extrusives and shallow intrusives.
iii. Plutonics.

According to IGME drilling the thickness of the marine sedimentary sequence within the basin is 250 m (cited in Innocenti et al., 1984).

Submarine extrusive and intrusive magmatic activity took place within the basin during late Eocene-Oligocene times.

There are no indications of continental volcanicity. Volcanic rocks occur mainly in the central and western part of the basin (Nea Santa, Mavropetra etc.). Volcanic and intrusive rocks are of acidic and intermediate composition and are represented by rhyolite, rhyodacite, dacite and andesite. K/Ar ages determined on selected samples from different Cenozoic basins, show that the volcanic activity in western Rhodope occurred mainly during the Oligocene. An age of 30.0±0.8 Ma was found for the volcanics of the Kirki-Essimi basin (Innocenti et al., 1986).

In the Kirki-Essimi area plutonic rocks occur both in the Late Eocene volcanosedimentary basin and intruded in the adjacent metamorphic basement. They form a series of monzonitic to granodioritic plutonic masses in a belt aligned approximately SW-NE, the principal outcrop occurs in the vicinity of Leptokarya.

2. SAMPLE COLLECTION - MEASUREMENT OF THE ANISOTROPY OF MAGNETIC SUSCEPTIBILITY.

Both oriented hand-samples and field-drilled cores have been utilized for the purposes of this study. The location of the sampling sites are illustrated in Fig.1. At each site, the freshest, unaltered parts were chosen for sampling and efforts were made to avoid faults, shear zones and slumped beds.

Three oriented hand-samples were collected from each site, large enough to extract at least three drillcores 2.54 cm in diameter and 5-6 cm in length, from which standard cylindrical specimens could be cut. This procedure ensures that an adequate number of specimens is available from each site, in order to apply the necessary statistical procedures and achieve a reliable overall result. A triangular perspex table incorporating two mutually perpenticular spirit levels was used for the orientation of these samples and the accuracy of orientation is normally between ±2°-4° (Collinson, 1983).

Field-drilled cores form the major part of the sample collection. Orientation of these cores was achieved by using a standard core orientation table (Tarling, 1971). It is estimated that these cores are oriented to an accuracy of ±2°-3° (Collinson, 1983). An effort has been made to collect at least three groups of cores from different positions on the outcrop to constitute a site.

Magnetic bearing measurements were taken using a magnetic compass, whilst a sun compass was also used in the majority of the cases. Measurement of the shadow angle, later enabled the calculation of the true bearing by utilizing a computer program, also using the date and time when the measurement was obtained, and the latitude and longtitude of the site locality (Collinson, 1983). The calculated true bearing values were found to be in very good agreement with the magnetic bearing values (corrected for the present declination of the Earth's field in the area), the maximum difference being about ±3°. It is thus suggested that the magnetic bearings can be used for the necessary corrections.

At least three drillcores were extracted from each oriented hand-sample, using a standard laboratory core drilling system.

Normally two specimens were cut from each of these cores as well as the ones collected in the field as previously described. In order to minimize errors due to specimen shape effects in anisotropy measurements a length/diameter ratio of 0.80-0.90 was adopted, as suggested by Noltimier (1971).

The strike and dip of each sampled sedimentary unit were measured in the field and subsequently a correction for tectonic tilt was made.

Highly sensitive instruments are required, in order to accurately measure the anisotropy of magnetic susceptibility. For sediments the Low Field Torque Magnetometer (LFTM) (King and Rees, 1962) is the most commonly used in measuring directly susceptibility differences, rather than the magnitude of the individual susceptibility axes. The different types of the currently available instruments for measuring the magnetic fabric of rocks, together with their respective sensitivity and accuracy, are reviewed by Hrouda (1982).

The low field torque magnetometer (LFTM) has been used throughout this study to measure magnetic fabric. King and Rees (1962) discuss in detail the construction and operation of this instrument. Essentially, a perspex sample carrier, suspended on a vertical torsion fibre, hungs at the centre of a vertical Helmholtz pair. The coils are mounted on a stage that can be rotated up to 180° about a vertical axis. A tuned alternating field (50 Hz) is produced by the coils and can be varied from 0.0 to 100.0 Oersteds.

When a sample is at the center of the coils, the field will induce a moment along the direction of maximum susceptibility in the horizontal plane of the sample. The induced moment will be deflected into the direction of the applied field by the influence of a torque T (King and Rees, 1962):

$$T = 1/2 \cdot v \cdot H \cdot (k_1 - k_2) \cdot \sin 2\theta \qquad (1)$$

where: v is the specimen volume, H is the field's strength, θ the orientation of coils, and k_1 and k_2 the two principal axes of susceptibility in the plane of measurement at right angles to each other.

The induced moment will follow the alternating field, but since the maximum axis is "double ended", T will be in the same sense throughout the alternating cycle. Thus, the net torque due to remanence component is zero, however, since during each half cycle the sense of rotation is equal and opposite, arresting any contribution it makes to the total deflection. Deflections are measured using a standard optical lever, where a light spot is reflected from a mirror affixed to the sample carrier onto a graduated scale. Five deflections are measured (with the Helmholtz coils oriented at 0°, 45°, 90°, 135° and 180°) for each of three orthogonal planes, giving a total of fifteen deflection values, which are sufficient to outline three torque curves. Details concerning the operation of the LFTM, as well as the calibration procedures are given by Hounslow (1984).

The deflections in each plane of measurement are deduced according to the following equations:

$$F_i = ((D_0 + D_{180})/2 - D_{90})/4 \qquad (2)$$

$$G_i = (D_{45} - D_{135})/2 \qquad (3)$$

where i is x, y or z depending on the plane of measurement and D are the deflections at coil azimuths of 0°, 45°, 90°, 135° and 180°. The parameters %G% (King and Rees, 1962) and Mean Amplitude (MA) (Hounslow, 1984) can also be used in order to

investigate the relevant dominance of the sin2θ component over other harmonics.

$$\Sigma G\% = (\Sigma G_i / MA) * 100 \quad (4)$$

where the mean amplitude is given by:

$$MA = [(F_i^2+G_i^2)/4]^{1/2} /3 \quad (5)$$

In this study specimens with MA<0.050 cm and/or ΣG%>100 (Spais, 1987), were rejected as too weak to provide reliable data or unreliably measured.

The plane which contains the k_{max} and k_{int} axes is defined as the magnetic foliation plane, and the k_{max} axis is the magnetic lineation. The use of various parameters has been proposed in order to compare the relative strength of lineation and foliation and also evaluate the degree of anisotropy exhibited by the various specimens (Hrouda, 1982). In this study the following parameters have been adopted:

$$LIN = (k_{max}-k_{int}) / k_{mean} \quad (6)$$

$$FOL = ((k_{max}+k_{int})/2-k_{min})/k_{mean} \quad (7)$$

$$q = LIN/FOL = (k_{max}-k_{int})/(k_{max}+k_{int})/2-k_{min}) \quad (8)$$

$$h\% = ((k_{max}-k_{min})/k_{min})*100 \quad (9)$$

The azimuthal anisotropy quotient "q" (Rees, 1966) varies from 0.0 for pure foliation to 2.0 for pure lineation, whilst the strength of anisotropy is measured by the percent anisotropy (h%) parameter, which is very useful in comparing the degree of alignment in a general sense, between two specimens with similar magnetic mineralogies. For sediments, the value of this parameter is generally less than 10 (Hamilton and Loveland, 1967). As suggested by Crimes and Oldershaw (1967), it is usual to refer to the angle between the k_{min} direction and the palaeovertical as "f-angle".

Subsequently specimens exhibiting q>0.670 and/or f>30° were rejected from the palaeocurrent estimation as they do not appear to possess a primary-style Anisotropy of Magnetic Calculation of the principal susceptibilities and their directions, together with parameters q, h%, LIN, FOL, ΣG% and MA, from the deflection data and the bulk susceptibility of each specimen was carried out by using program "ANIS2" on a Hewlett-Packard HP86 computer.

In order to reduce the instrumental noise effects a "holder correction" (Hounslow, 1984) was applied on all data. Measurement of the anisotropy of the perspex holder used are regarded as defining a weak sin2 curve, which is subsequently subtracted from the sample curve in order to improve the approximation of the magnetic fabric of the sample. For the specimens of the present study though, no appreciable difference is revealed for the directions of the principal axes of the susceptibility, even for very weakly anisotropic specimens.

All directional magnetic fabric data for this study are conventionally represented by the orientations of the k_{max} and k_{min} axes plotted on the upper hemisphere of an equal area projection. Plotting of the k_{int} axis was omitted on the basis that its direction can always be determined from the two other principal susceptibility axes, since the three axes are orthogonal. Additionally rose diagrams of the k_{max} azimuths plotted at a class interval of 10° are presented for all individual sites to better aid the visual identification of any preferred directional trends.

Since two individual LFTMs, were used during the course of

this study, one in the Geology and the other in the Oceanography Department intercalibration of the two instruments was carried out by measuring a selection of 10 specimens using both instruments and by subsequently comparing both the directional as well as the magnitude data. The results are in very good agreement for all .specimens suggesting that data obtained on either of the two instruments is identical (Spais, 1987).

In order to calculate mean directions of the principal susceptibility axes for individual layers and sites Fisher (1953) statistics was applied for the k_{min} axes. Since the k_{max} are more or less co-planar producing an almost two-dimensional distribution Von Mises statistics (Mardia, 1972) was applied in this case in order to calculate mean trends and their associated error (Circular Standard Deviation) parameters.

3. RESULTS PRESENTATION AND DISCUSSION.

The azimuthal anisotropy quotient (q) (Rees, 1966) is considered as a very sensitive indicator of the character of the magnetic fabric possessed by a specimen. A number of previous studies sought to try to define various limits on this parameter as a means of identifying different conditions and/or environments of sedimentation (Hamilton, 1967; Hamilton and Rees, 1970; Rees and Woodall, 1975; Frederick, 1972). Values of q ranging between 0.06 and 0.42 were suggested for sediments formed by grain-by-grain deposition onto a flat surface, whilst higher values ranging between 0.43 and 0.67 are considered as more representative for sediments deposited by avalanching down angle of repose slopes. Lower values ($0.06<q<0.21$) were suggested for still water sedimentation on sloping beds.

In this study the value of 0.67 was adopted as an upper limit for q, but no further classification of its values has been attempted, apart from limited speculation concerning the sedimentation environment at different locations within the basin. Hence, all specimens with q values lower than this limit are considered as possessing primary style magnetic fabric and thus inherently provide important information about any prevailing palaeocurrent direction during their deposition.

Some interesting conclusions can be drawn from a study of magnetic fabric results from site ES21 and possibly generalized for the rest of the basin sites. The mean h% and q values for the sampled layers of sites ES20 and ES21 are illustrated in Fig.2.

Application of the bedding correction contributes to both the improvement of the clustering of the kmin axes as well as to the restoration of the k_{min} axes near to the palaeovertical (Fig.3). It does thus provide conclusive evidence that the magnetic fabric under study is of primary origin and predates the tectonically-related tilting for which the bedding correction was applied. Especially for sites ES20/21 it also suggests that no further major within-site folding has affected the sites. Fig.4 illustrates the orientation of the susceptibility axes for the sampled in detailed site ES21.

The similar palaeocurrent trends inferred for the arbitrary division of site ES21 into three parts (as illustrated in Fig.5) suggests that no major change in palaeocurrent direction occurred during the infilling of the basin, at least in its central part, for the time-span covered by the sampled sedimentary interval.

Primary style magnetic fabric is exhibited by the rest of the sites within the Kirki-Essimi basin, except site ES13, which exhibits a deformational style magnetic fabric. Typical examples are demonstrated by Figures 6,7,8,9 and 10 for sites ES04, ES05, ES12, ES14 and ES16 respectively.

Site ES13 is the only individual site within the basin showing totally deformational-style fabrics. Specimens exhibit comparatively low h% values (1.66±0.20). The extremely high q values (1.522±0.088) combined with the shallow k_{min} axes orientation (f>86°), strongly suggest a deformational style fabric. Fig.9 demonstrates the close grouping of the kmax axes about a direction of Dec=126.1°, Inc=-48.4°, a_{95}=3.3°), while kmin directions appear to girdle within a plane normal to the kmax direction. This suggests that the deformational-style fabric observed was produced by a stress aligned along a NNE-SSW trend (at 36°E).

Primary style magnetic fabric is exhibited by the Drymou-Melias sites DM18, DM19 and DM20 and thus palaeocurrent directions are deduced for these sites. The orientations of the K_{max} and k_{min} axes for site DM18 are illustrated in Fig.12 together with the inferred palaeocurrent direction. The h% and q parameters for the Drymou-Melias sites are compared to those of the Kirki-Essimi basin sites, a similar range of values are derived for both h% and q. The distribution of h% values appears to be somewhat broader in the case of the Drymou-Melias sites compared to the Kirki-Essimi sites, whilst very similar sedimentation conditions for both groups are suggested by closely similar distribution of q values.

In terms of inferred palaeocurrent directions an almost southerly palaeocurrent trend is suggested for sites DM18 and DM22, in contrast to an easterly one deduced for site DM19 situated near to the southern margin of the Drymou-Melias series. There is also a significant difference of about 30° between the palaeoflow directions inferred for the first two sites, although they are only a few meters apart.

The strong near horizontal magnetic foliation exhibited by all sites (except ES13) is considered as an indication of the dominance of gravitational orienting couples during basin infilling. It can also be stated that for the Kirki-Essimi basin sites there is no evidence of extensive alteration, and bioturbation is absent. Thus no post-depositional modification to the fabric (Ellwood, 1984) is likely from these sources.

No estimation of palaeocurrent directions using any other conventional sedimentological method, has been attempted before for the whole, or part, of the sedimentary sequence of the Kirki-Essimi basin. Therefore, the reliability of the inferred palaeocurrent direction from this magnetic fabric study, cannot be directly evaluated by comparison to the results of any other independent technique. However, the usefulness of the method in deducing palaeocurrent trends can be appraised.

The palaeocurrent trends/directions inferred for each of the sites studied, are presented in Table 1 and illustrated in

Fig. 13. The small number of specimens rejected from the palaeocurrent calculation, together with the low error parameters (csd) associated with most of the sites, suggest that the technique can be successfully applied to the clastic sediment sequences of the basin in order to deduce palaeocurrent directions. Only 18% of the specimens measured had to be excluded from the analysis of the palaeocurrent directions and only about 50% of these actually exhibited deformational-style magnetic fabric; the rest being rejected on the basis of possessing weak magnetic fabric.

There appears to be a difference in palaeocurrent trends on either side of the prominent NW-SE striking fracture/fault system as indicated by the palaeocurrent directions inferred by sites ES10 and ES11 (particularly the latter, which is the only site suggesting a northerly directed palaeocurrent).

Relatively well-defined ($\alpha_{95} < 15.0$) stable remanence directions were obtained for sites ES02, ES04, ES11, ES12, ES14 and ES16. These remanence directions imply relative rotations if compared to the present Earth's field in the area. The palaeocurrent trends were subsequently corrected for the respective rotation deduced for each of these sites. For the rest of the sites large α_{95} values of up to 40°, do not allow application of similar correction.

Table 2 illustrates the corrected palaeocurrent direction for each of these sites, together with the magnitude of the correction, which is positive for the sites for which the originally inferred direction had to be rotated clockwise and vice versa. The corrected directions are also shown in the map of Fig. 14. Both Table 2 and Fig. 14 imply that corrections of the order of 40°-50°, are required for sites ES04 and ES11. Application of the correction significantly alters the inferred palaeocurrent directions, suggesting near longitudinal palaeocurrent directions for both sites. The overall palaeocurrent pattern previously established for the basin is therefore modified as a consequence probably suggesting a depositional fan environment. However, for the remaining sites to which similar correction was applied, it did not result in any significant change of the palaeocurrent trends deduced initially.

Analysis of the magnetic fabric results for the Kirki-Essimi basin indicates an episode, or episodes, of basin infilling dominated by sedimentation conditions giving rise to primary style fabrics. Two dominant palaeocurrent trends emerge (N-S) and (E-W). The (E-W) trend is typified by sites ES14, ES17 and ES20/21, which are situated in the middle and probably deepest part of the Kirki-Essimi basin and are closely associated with the occurrences of the stratiform sulphide mineralization. For sites ES14 and ES20/21 the mean transport direction indicates an unidirectional current flow, which is likely to represent a longitudinal (axial) flow direction within the basin.

For sites ES02, ES03, ES04 and ES05 , a southerly transport direction is implied (at least consistently for ES02, ES04 and ES05). An explanation for this can be sought in terms of transverse palaeocurrents flowing southwards away from the basin margins formed by the Rhodope crystalline basement to the north. In general terms it is possible to infer from these observations, that palaeoslopes may have existed to the north

and west of the present basin configuration. The configuration of such slopes would have had a controlling effect in determining the form of sediment transport into the basin. The fact that all sites for which axial palaeocurrent directions are inferred, are situated in the central part of the basin is considered to be an important feature of the palaeocurrent pattern within the basin.

The occurrence of two principal palaeocurrent trends, suggests the possibility that at different times during basin infilling, one or the other of these trends has been dominant. Alternatively, margin and axial transport directions may have co-existed. The latter appears to be a stronger possibility, particularly in the light of the results for sites ES20/21, which suggest that they constitute of a similar palaeocurrent trend throughout the time-span covered by the sampled 150 m of this sequence.

The secondary (deformational) style magnetic fabric exhibited by site ES13, can be attributed to a compressional stress aligned along a NNE-SSW trend. Whether this represents a general feature of the area, being associated to the N-S extension during basin evolution (Sanderson et al., 1986), or it reflects a more localized tectonic episode is not known. It is noted that the direction of the inferred stress is almost perpendicular to the present outcrop boundary between the Essimi volcanics and the adjacent sediments. As this site is in close proximity to this boundary, then it is also possible that its fabric was affected by localized stresses imposed by the extrusion of the Essimi volcanics. As the observed deformational magnetic fabric characteristics are compatible with both the N-S extension, which is a general feature of the basin area as well as the volcanicity in the Essimi area, it is very probable that they have both contributed to the resultant magnetic fabric.

The palaeocurrent directions inferred for sites ES16 and ES17, which are situated very close to the northern boundary of the basin sedimentary sequence with the metamorphic basement are aligned approximately perpendicular to the boundary. There is a real possibility here that sedimentation, at these sites, took place on a sloping surface, but this cannot be proved conclusively as there is no independent evidence as to the exact position of the northern boundary of the basin, or its form, during the basinal infilling phase.

Similar problems are encountered in the interpretation of the magnetic fabric exhibited by sites ES10 and ES11. The palaeocurrent directions appear to parallel the deep fracture/fault system (see Fig.13), which has probably affected the sedimentation regime in its vicinity, altering probably the local palaeobathymetry of the basin in this area. On the basis of q and f-angle values, the magnetic fabric of these sites is considered as primary and therefore the palaeocurrent directions deduced as realistic. After applying the rotation correction to site ES11, the resulting palaeocurrent direction is still incompatible with the directions inferred for the rest of the sites in this part of the basin. Therefore, it can be inferred that sediment transport in the vicinity of this major fault is strongly influenced by it.

Alternatively, taking an overview of the few well-determined palaeocurrent directions, excluding sites ES10 and ES11, it is possible that the pattern of transport directions

revealed by this study represents a depositional fan environment. Such a fan would be sourced in the north-northwest of the area and merge dictally to the south with axial transpport systems. The major fault-system transecting the basin, may itself have influenced the easterly and south-easterly margins of this fan, contributing to the slightly anomalous palaeocurrent direction shown by site ES12. Further speculation in the absence of other confirmatory sedimentological evidence is not warranted.

The directions inferred for sites DM18 and DM22, appear to be controlled by the two faults situated on either side of the sites. Unfortunately no well-defined stable remanence direction was obtained for either site, in order to appropriately correct for any rotation. The significantly different palaeocurrent directions deduced for these two sites might also be explained if unknown tectonic effects are not properly accounted for when applying the bedding correction.

The dominance of an easterly palaeoflow direction obtained for site DM19 could indicate bottom current transport out of the Kirki-Essimi basin towards another deeper basin situated to the east, both being marginal basins peripheral to the Tethys ocean. All these suggested interpretations are advanced on the basis of the present basin configuration. It is possible that this configuration might have been very different when sedimentation took place in Eocene times and it is possible that all sites (including DM18, DM19 and DM22) were within the same basin. On the basis of the magnitude parameters h% and q, alone, it can be suggested that the Kirki-Essimi and the Drymou-Melias sites are very similar as far as their magnetic fabric is concerned.

4. CONCLUSIONS.

The very small percentage of specimens, which had to be rejected from palaeocurrent estimation is indicative of the success of the method as a means of palaeocurrent analysis for the clastic sedimentary sequence of the Kirki-Essimi basin. The vast majority of the specimens measured exhibited primary style depositional magnetic fabric, characterized by q and f-angle values smaller than 0.67 and 30°, respectively.

Almost 50% of the rejected specimens showed deformational style magnetic fabric, however only one site (ES13) exhibited entirely deformational magnetic fabric. The direction of the compressional stress inferred is generally compatible with the N-S extension suggested for the area. The magnetic fabric of this site could have also been partially affected by the intrusion of the neighbouring Essimi body.

The two main palaeocurrent trends emerging, a N-S and an E-W one, are mainly typified by sites situated in the western and central parts of the basin respectively. On the basis of the results for sites ES20 and ES21 from which no significant change in palaeocurrent trend is suggested throughout the sampled 150 m, it appears that these two trends co-existed rather than one of the two being dominant at different times during basin infilling. Such palaeocurrent may have been related to the existence of palaeoslopes at the north and west of the present basin configuration.

An alternative palaeocurrent pattern results by taking into account the relative rotations of the sites as suggested by the palaeomagnetic results. This can be interpreted to suggest a depositional fan environment. The fan would have its source situated in the north-northwest of the area and merge distally to the south with axial transport systems.

The approximate easterly palaeoflow directions deduced for sites DM18 and DM19 may indicate bottom current transport out of the Kirki-Essimi basin and probably towards another deeper basin, both being peripheral to the Tethys ocean. However, the limited number of sites does not allow a preferred differentiation between the two models.

In the light of the results of the present study it is suggested that local fluctuations of palaeocurrent trends in the vicinity of the mineralized area to the north-east of Essimi (towards the Prophetis Elias region) can be studied further. This will require more extensive sampling in that part of the basin. Most importantly though, the difference in palaeocurrent trend recognized on either side of the main fault system, should certainly be better established. Extensive sampling in the eastern and north-eastern part of the basin is a prerequisite for any such attempt.

REFERENCES

Aziz-ur-Rahman, Gough, D.I. and Evans, M.E., 1975: Anisotropy of magnetic susceptibility of the Martin Formation, Sascatchewan and its sedimentological implications.
Can. J.Earth Sci., 12(8), 1465-1475.

Billett, M.F. and Nasbitt, R.W., 1986: Base-metal mineralization associated with mafic and ultramafic rocks, eastern Rhodope massif, Greece.
Trans. Ins. Min. Metall., 95, B37-B45.

Collinson, D.W., 1983: METHODS IN ROCK MAGNETISM AND PALAEO-MAGNETISM, Chapman and Hall, London.

Crimes, T.P. and Oldershaw, M.A., 1967: Palaeocurrent determinations by magnetic fabric measurements of the Cambrian rocks of St. Tudwal's Peninsula, North Wales.
Geol. J., 5(2), 217-232.

Elwood, B.B., 1984: Bioturbation; minimal effects on the magnetic fabric of some natural and experimental sediments.
Earth Planet. Sci. Letters, 67, 367-376.

Fisher, R.A., 1953: Dispersion on a sphere.
Proc. R. Soc. (London), A217, 295-305.

Frederick, D., 1972: The magnetic fabric of some recent merine sediments.
Ph.D. Thesis (unpublished, University of Southampton.

Hamilton, N., 1967: The effect of magnetic and hydrodynamic control on the susceptibility anisotropy of redeposited silt.
J. Geol., 75, 738-743.

Hamilton, N. and Loveland, P.J., 1967: Some preliminary susceptibility anisotropy measurements on greywackes from the Trinity peninsula series of Graham land.
Br. Antarct. Surv. Bull., 11, 59-71.

Hamilton, N. and Rees, A.I., 1970: The use of magnetic fabric in palaeocurrent estimation.
In Runcorn, S.K. (Ed.): Palaeogeophysics, Oxford, 445-463.

Hamilton, N. and Rees, A.I., 1971: The anisotropy of magnetic susceptibility of the Franciscan rocks of the Diablo Range, Central California.
Geol. Rundsch., 60, 1103-1124.

Hounslow, M.W., 1984: Sedimentological implications of magnetic fabric measurements of some Jurassic and Late Triassic sediments.
Ph.D. Thesis (unpublished), University of Southampton.

Hrouda, F., 1982: Magnetic anisotropy of rocks and its application in geology and geology.
Geophysical Surveys, 5, 37-82.

Innocenti, F., Kolios, N., Manetti, P., Mazzuoli, R., Peccerillo, G., Rita, F. and Villari, L., 1984: Evolution and geodynamic significance of the Tertiary orogenic volcanism in Northeastern Greece.
Bull. Volcanol., 47, 25-37.

Jacobshagen, V., 1977: Structure and geotectonic evolution of the Hellenides.
VI Col. on the Geology of the Aegean region, Athens, 1355-1367.

Katirtzoglou, C., Bitzios, D., Demetriades, A. and Constantinides, D., 1981: Late Alpine polymetallic mineralization at the southern margin of Rhodope (Essimi district), Greece.
Internal Report, I.G.M.E., Athens (Greel text).

King, R.F. and Rees, A.I., 1962: The measurement of the anisotropy of magnetic susceptibility of rocks by the torque method.
J. Geophys. Res., 71, 561-571.

Mardia, K.V., 1972: STATISTICS OF DIRECTIONAL DATA.
Academic Press, London.

Noltimier, H.C., 1971: Magnetic rock cylinders with negligible shape anisotropy.
J. Geophys. Res., 75, 4035-4037.

Papanikolaou, D., 1984: The three metamorphic belts of the Hellenides: A review and a kinematic interpretation.
In Dixon, J.E. and Robertson, A.H.F.(Eds.): The geological evolution of the Eastern Mediterranean, Geol. Soc. Lond. special publication No 17, 551-561.

Rees, A.I., 1966: The effect of depositional slopes on the anisotropy of the magnetic susceptibility of laboratory deposited sands.
J. Geol., 74, 856-876.

Rees, A.I., Von Rad, U. and Shepard, F.P., 1968: Magnetic fabric of sediments of the La Jolla submarine canyon and fan, California.
Marine Geol., 6, 145-178.

Rees A.I. and Woodall, W.A., 1975: The magnetic fabric of some laboratory deposited sediments.
Earth Planet. Sci. Letters, 25, 121-130.

Sanderson, D., Benton, M., Spence, J., Billett, M., Nesbitt, R.W., Karfakis, Y., Tsombos, P., Archer, P. and Legg, C., 1986: Application of remote sensing to an investigation of structural controls of mineralization in the eastern Rhodope massif.
Final Report for the E.E.C. project: New concepts in mineral exploration philosophy and their use in the study of polymetallic mineralization in the Rhodope region, Greece.
Brussels.

Spais, C., 1987: Palaeomagnetic and magnetic fabric investigations of Tertiary rocks from the Alexandroupolis area, N.E. Greece.
Ph.D. Thesis (unpublished), University of Southampton.

Tarling, D.H., 1971: Gondwanaland, palaeomagnetism and continental drift.
Nature, 229, 17-21.

Von Rad, U., 1971: Comparison between magnetic and sedimentary Fabric inGraded and Cross-laminated Sand layers, Southern California.
Geol. Rundsch., 60, 331-354.

---

[1] Present Address: Themistokleous 75, Neo Psihiko, 154 51 Athens, GREECE.

LIST OF TABLES

Table 1

Palaeocurrent and mean k_{min} directions for the Kïrki-Essimi basin and the Drymou-Melias sites.

SITE CODE	PC DIRECTION Trend	^{o} E	(csd)	Mean K_{min} Dec / Inc (α_{95})	N / N_o (%rej)
ES02	S	186.5	(6.8)	341.4 / -80.4 (14.7)	4 / 14 (71.4)
ES03	S-SW	209.4	(6.4)	352.1 / -83.5 (14.2)	5 / 9 (44.4)
ES04	S-SW	194.1	(13.9)	038.0 / -84.2 (7.5)	14 / 14 (0.0)
ES05	S-SW	203.2	(14.6)	319.3 / -75.9 (3.3)	14 / 14 (0.0)
ES10	NW-SE	148.6	(17.5)	058.8 / -83.0 (4.8)	11 / 11 (0.0)
ES11	N-NW	335.2	(11.6)	117.0 / -76.9 (7.0)	11 / 11 (0.0)
ES12	S-SW	199.1	(5.6)	052.8 / -81.1 (5.1)	10 / 10 (0.0)
ES14	E-SE	107.2	(5.1)	264.7 / -84.5 (3.9)	10 / 10 (0.0)
ES16	S-SE	148.7	(10.6)	289.4 / -80.5 (5.0)	8 / 9 (11.1)
ES17	E-SE	106.3	(12.2)	278.0 / -79.8 (7.5)	9 / 9 (0.0)
ES20	NE	55.6	(13.3)	254.6 / -83.6 (3.8)	16 / 16 (0.0)
ES21	NE	49.1	(16.8)	259.4 / -85.1 (2.0)	93 /109 (14.7)
DM18	S-SE	165.1	(20.3)	314.8 / -83.5 (4.1)	34 / 51 (31.4)
DM19	E-SE	102.5	(19.5)	345.3 / -85.0 (2.9)	46 / 54 (14.8)
DM22	S-SW	195.4	(5.1)	069.3 / -79.6 (3.9)	11 / 13 (15.4)

Table 2

Corrected palaeocurrent directions.

SITE CODE	CORRECTED PALAEOCURRENT DIRECTION (° E)	APPLIED CORRECTION(°)
ES02	193.1	+ 6.9
ES04	244.0	+ 47.0
ES11	292.9	- 42.3
ES12	192.4	- 6.9
ES14	103.3	- 3.8
ES16	146.7	- 2.0
ES17	94.8	- 11.5
DM18	113.1	- 52.0
DM19	35.8	- 66.7

Positive differences: Clockwise correction
Negative differences: Anti- " correction

LIST OF FIGURES

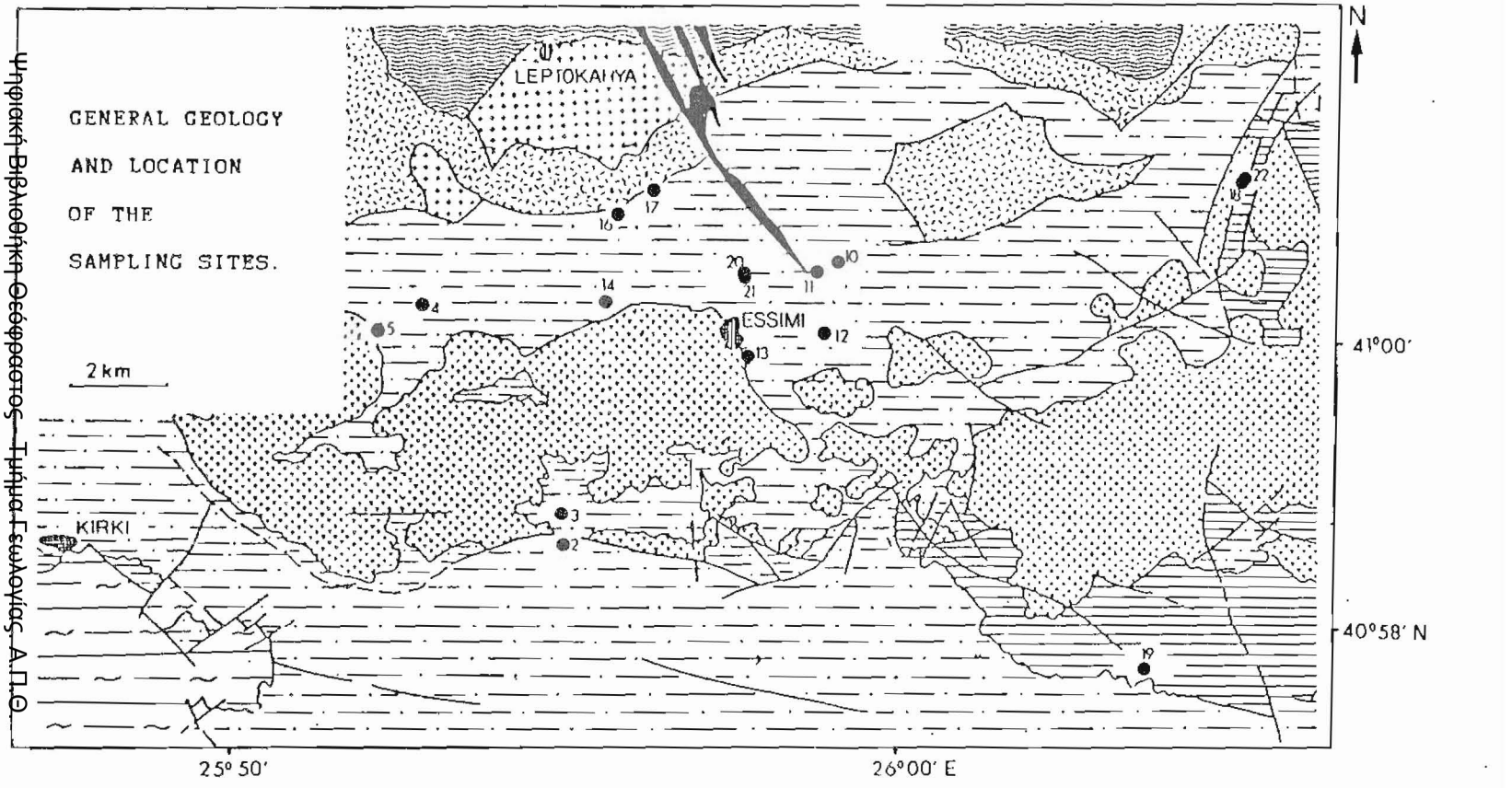

LEGEND (Fig. 1)

Rhyolites, dykes of rhyolitic-rhyodacitic composition (Oligocene-Miocene?)

Dacites and andesites with alterations of pyroclastics (Upper Eocene). Intrusive formations and dykes (Oligocene).

BASIC CLASTIC SERIES Limestones (Lutetian), flysh series (Priabonian) clayey-marly series (Oligocene), marine facies deposits (Miocene).

PLUTONIC FORMATIONS granodiorites, monzonites, monzodiorites, quartz diorites and diorites.

Dolerites, spilites and pyroclastic of basic composition

DRIMOU-MELIAS SERIES (Jurassic-Lower Cretaceous) Sedimentary rocks with strong diagenesis.

PHYLLITE SERIES Argillaceous, sericitic schists, quartzites, marbles & sandstones.

Metamorphic, basic and ultrabasic rocks.

Gneisses, muscovite schists, granitic schists and augen-gneisses.

fault

geological boundary

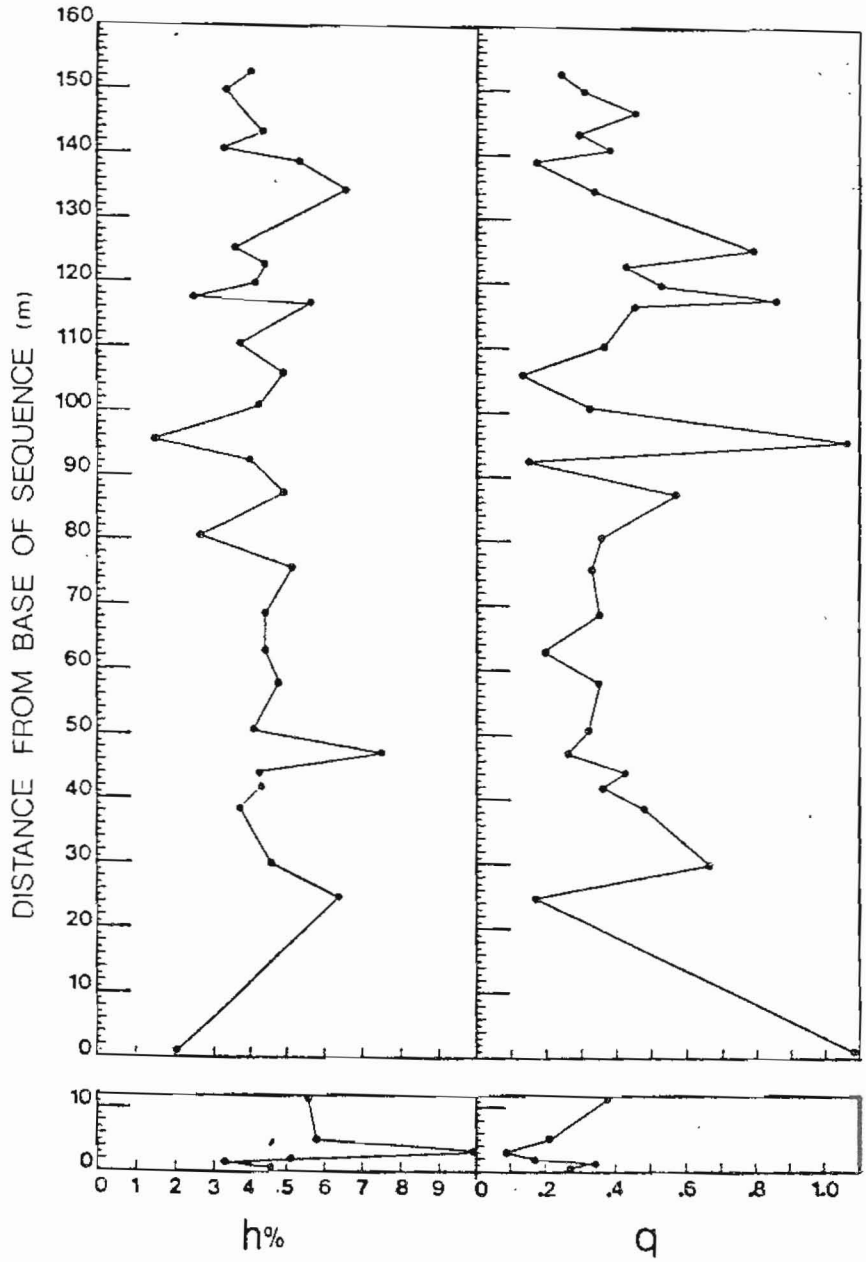

Fig. 2: Mean h% and q values for the sampled layers of sites ES20 and ES21.

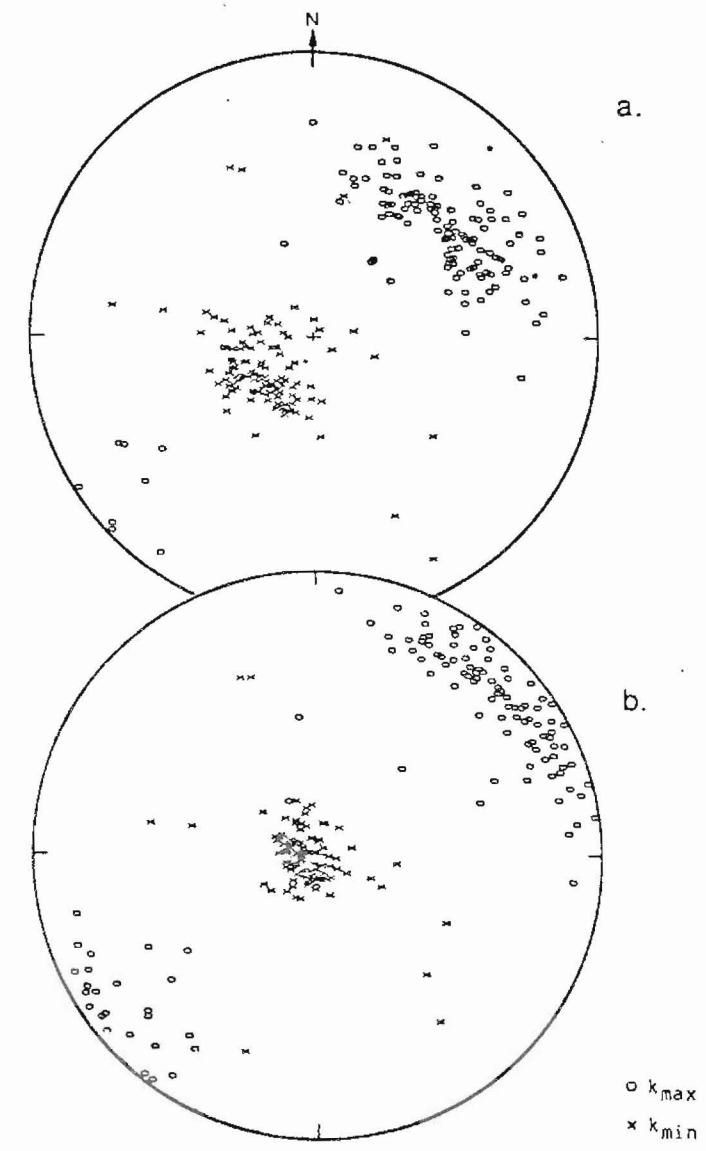

Fig. 3: Orientation of susceptibility axes for all specimens from sites ES20 and ES21:
(a) before and (b) after bedding correction.

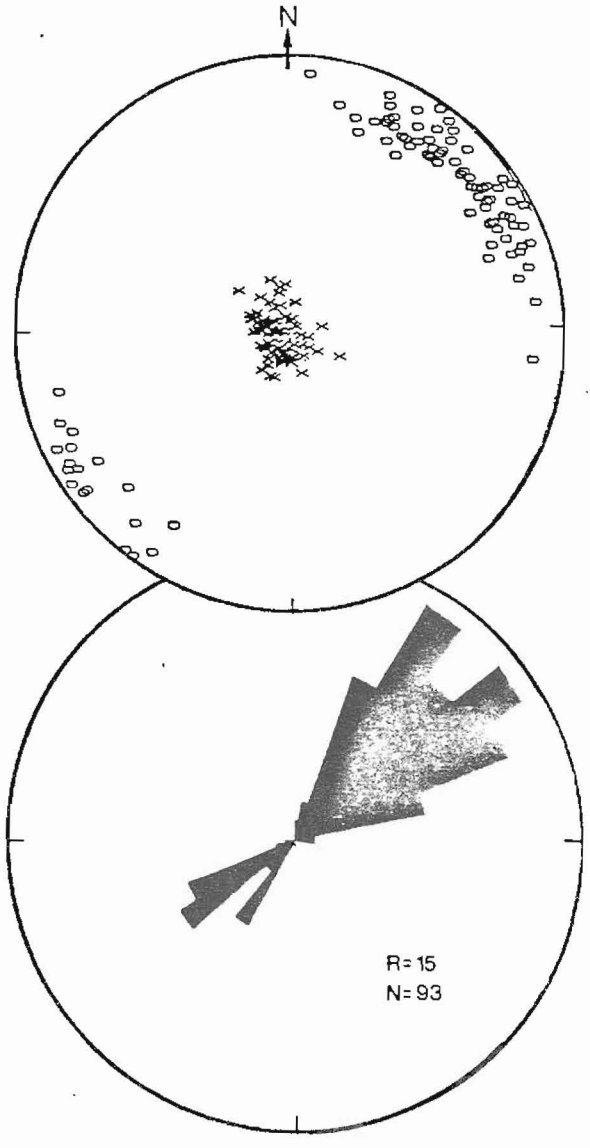

Fig. 4: Site ES21
Specimens exhibiting primary style magnetic fabric (a) orientation of susceptibility axes, (b) orientation of k_{max}-axes declination.

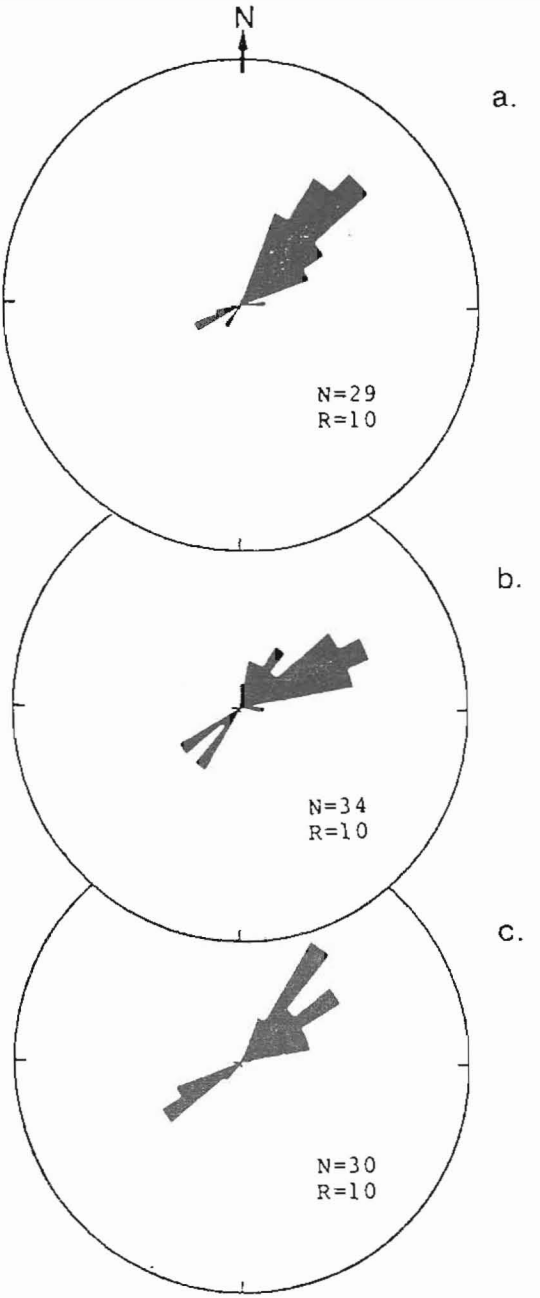

Fig. 5: Site ES21
Orientation of k_{max}-axes declination for specimens from: (a) layers ES21.01 - ES21.10, (b) layers ES21.11 - ES21.20, (c) layers ES21.21 - ES21.32.

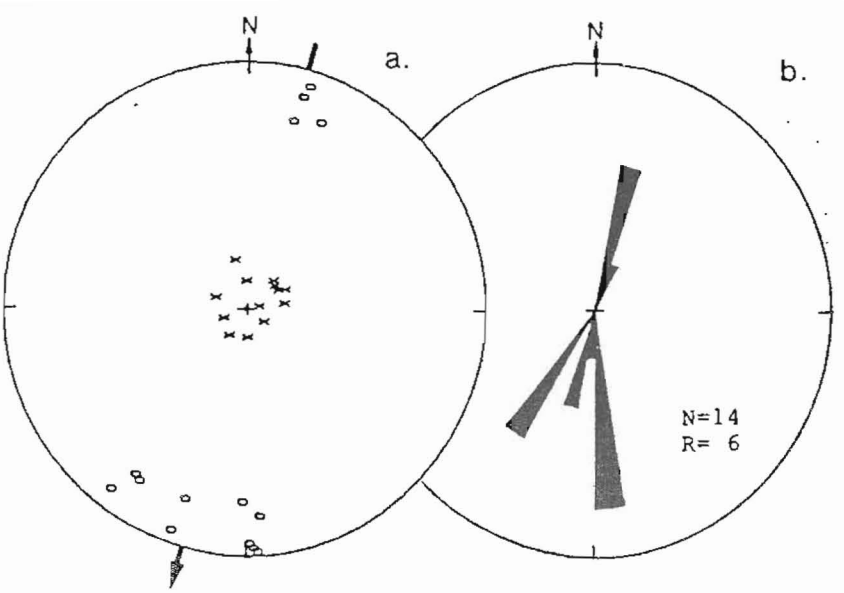

Fig. 6: Site ES04 - All specimens:
(a) susceptibility axes orientation,
(b) Orientation of k_{max}-axes declination.

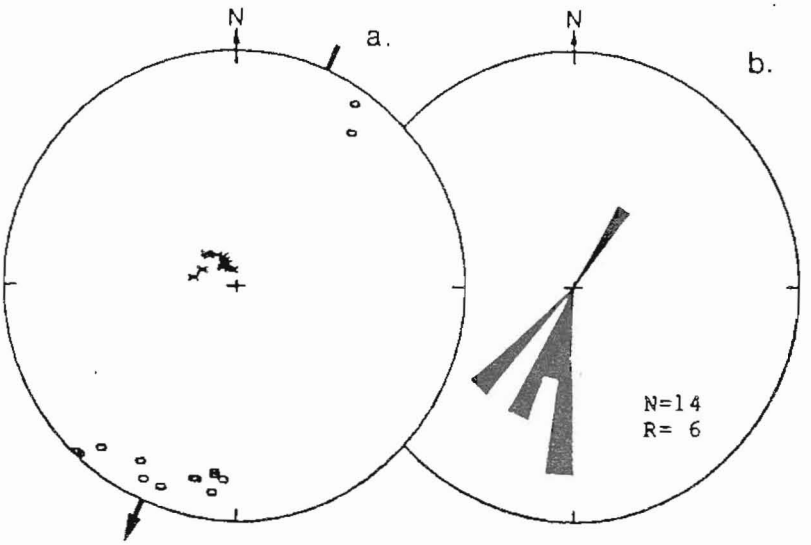

Fig. 7: Site ES05 (Caption as in Fig.6)

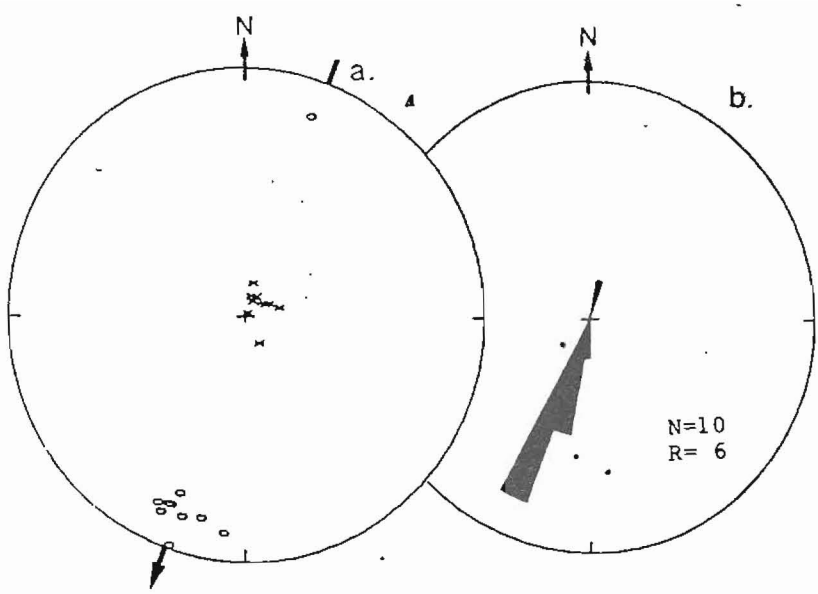

Fig. 8: Site ES12 (Caption as in Fig.6)

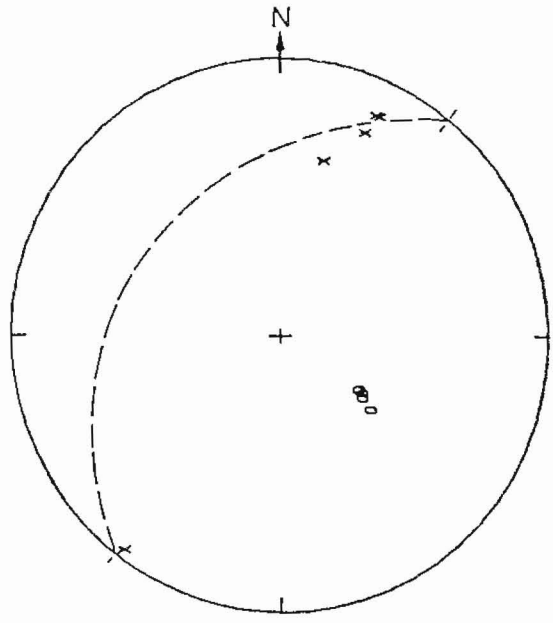

Fig. 9: Site ES13: Susceptibility axes orientation for all specimens.

The dashed line represents the plane normal to the mean K_{max} axis.

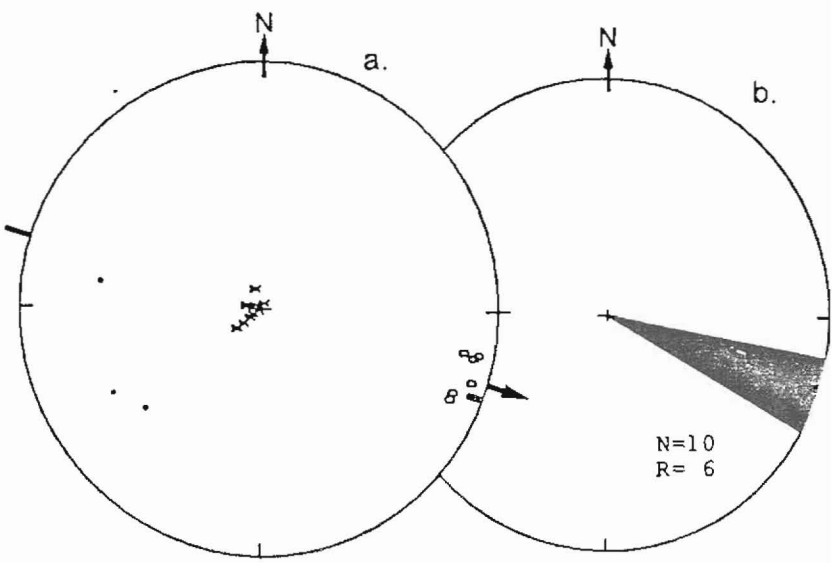

Fig.10: Site ES14 (Caption as in Fig.6)

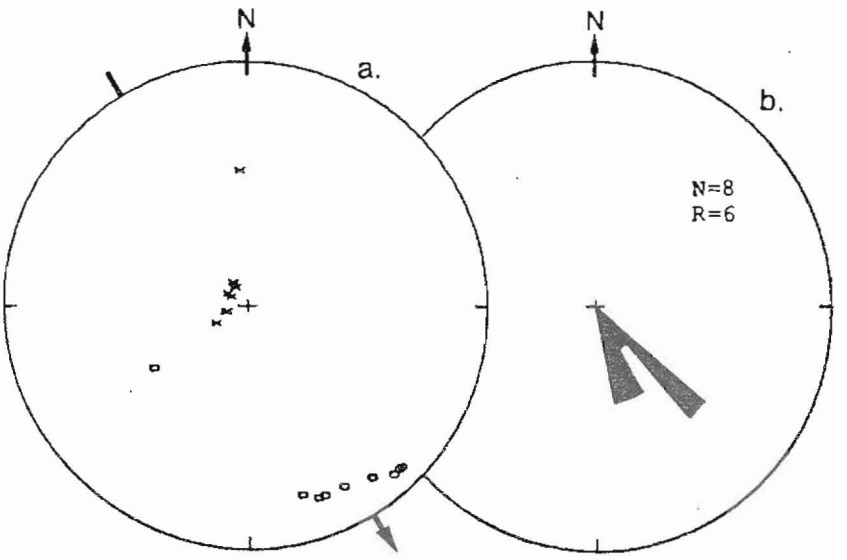

Fig.11: Site ES16 (Caption as in Fig.6)

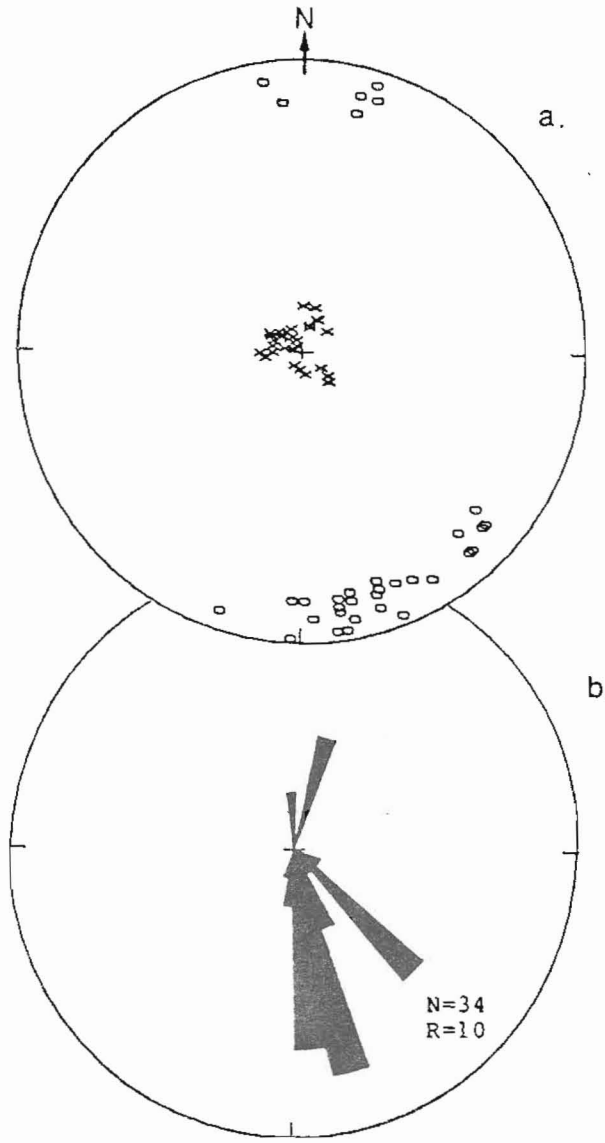

Fig.12: : Site DMI8: Specimens exhibiting primary style magnetic fabric:
(a) orientation of susceptibility axes, and
(b) orientation of kmax-axes declination.

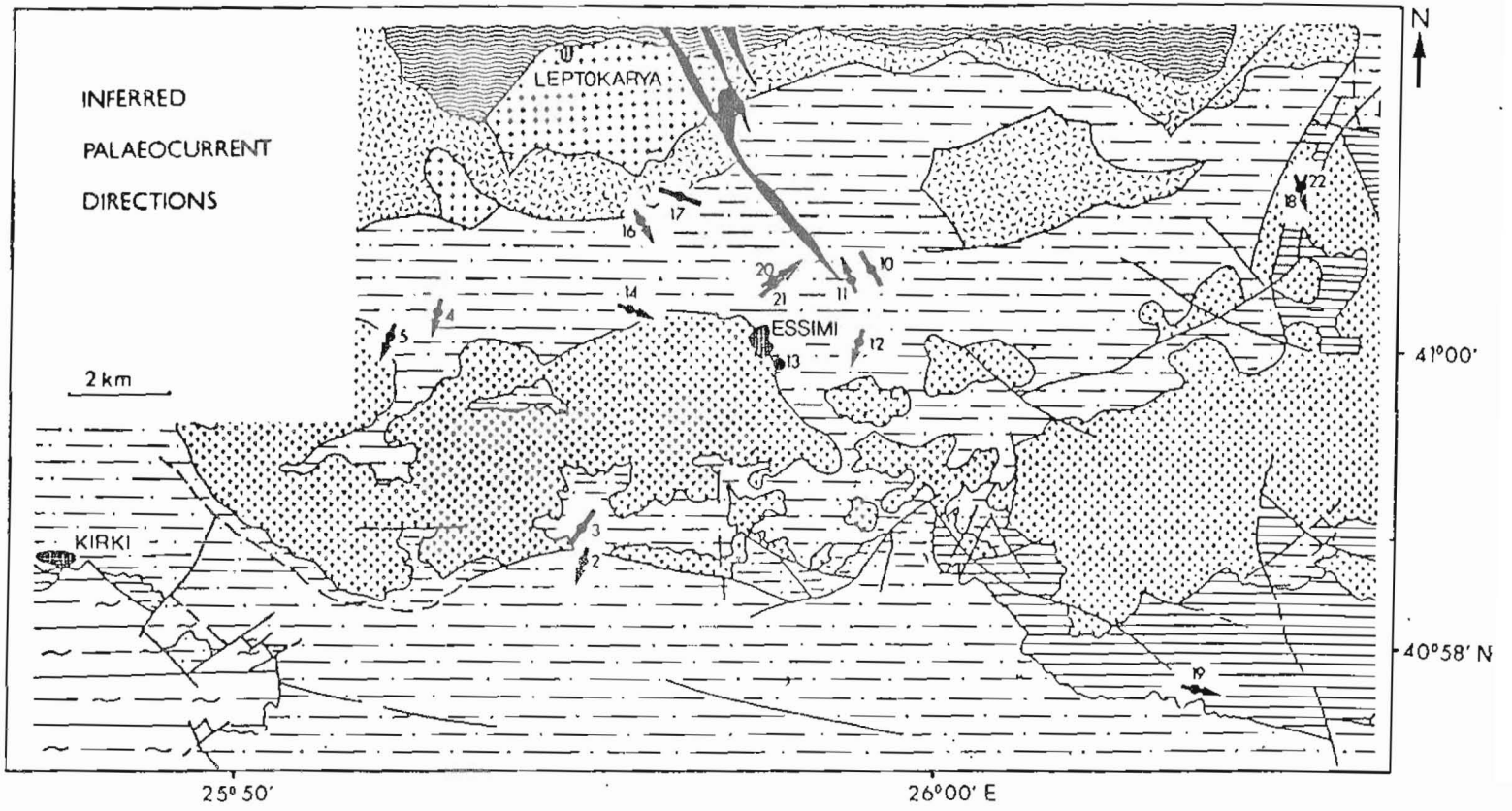

Fig. 13: Inferred palaeocurrent directions for all sites.

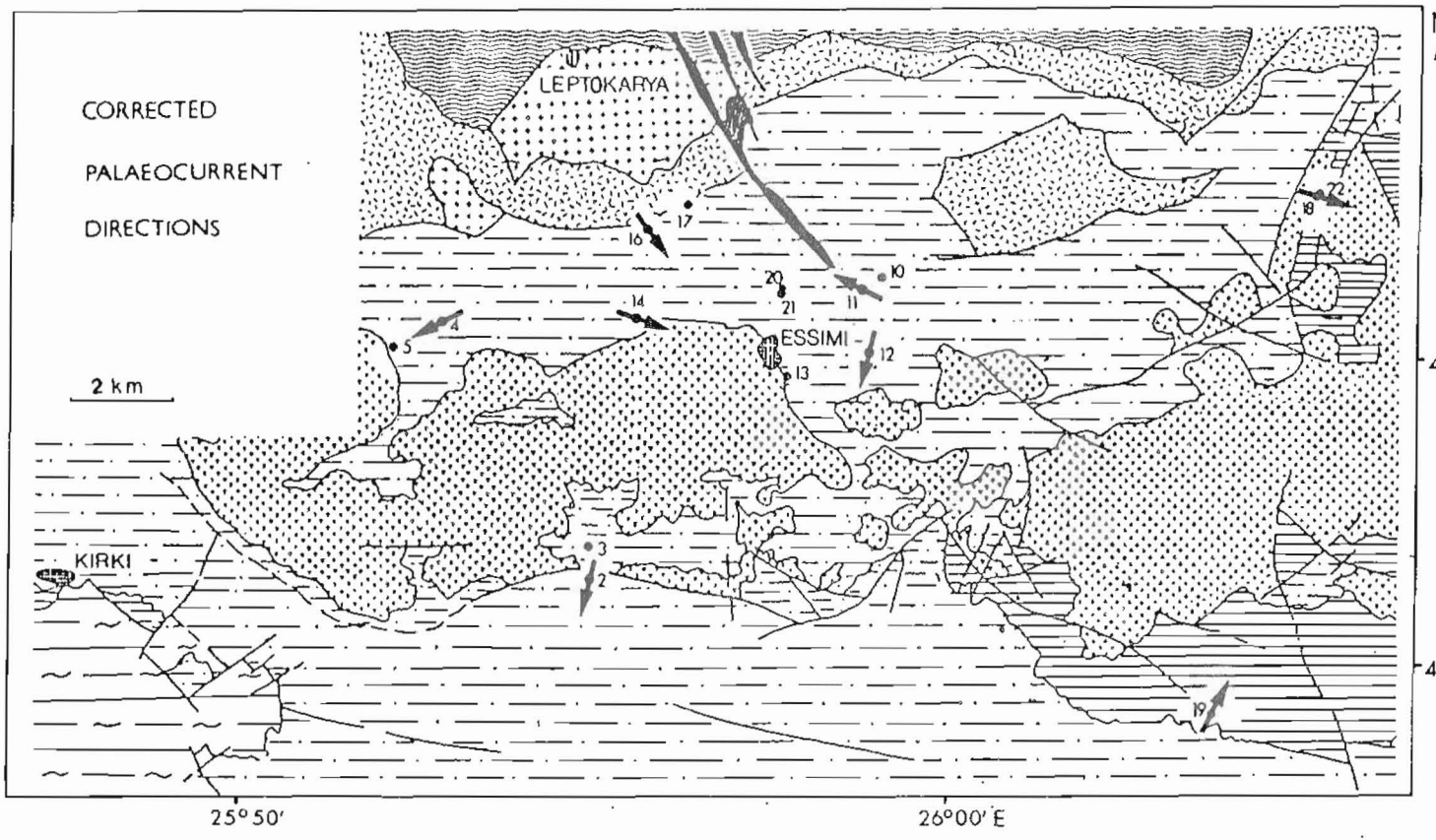

Fig. 14: Palaeocurrent directions emerging after application of the rotation correction.